Journal of
Mechanics of
Materials and Structures

OPTIMAL BUCKLING DESIGN OF ANISOTROPIC RINGS/LONG CYLINDERS UNDER EXTERNAL PRESSURE

Karam Y. Maalawi

Volume 3, № 4 April 2008

mathematical sciences publishers

JOURNAL OF MECHANICS OF MATERIALS AND STRUCTURES
Vol. 3, No. 4, 2008

OPTIMAL BUCKLING DESIGN OF ANISOTROPIC RINGS/LONG CYLINDERS UNDER EXTERNAL PRESSURE

KARAM Y. MAALAWI

Structural buckling failure due to high external hydrostatic pressure is a major consideration in designing rings and long cylindrical shell-type structures. This paper presents a direct approach for enhancing buckling stability limits of thin-walled rings/long cylinders that are fabricated from multiangle fibrous laminated composite lay-ups. The mathematical formulation employs the classical lamination theory for calculating the critical buckling pressure, where an analytical solution that accounts for the effective axial and flexural stiffness separately as well as the inclusion of the coupling stiffness terms is presented. The associated design optimization problem of maximizing the critical buckling pressure has been formulated in a standard nonlinear mathematical programming problem with the design variables encompassing the fiber orientation angles and the ply thicknesses as well. The physical and mechanical properties of the composite material are taken as preassigned parameters. The proposed model deals with dimensionless quantities in order to be valid for thin shells having different thickness-to-radius ratios. Useful design charts are given for several types of anisotropic rings/long cylinders showing the functional dependence of the buckling pressure on the selected design variables. Excellent results have been obtained for cases of filament wound rings/long cylinders fabricated from three different types of materials: *E*-glass/vinyl-ester, graphite/epoxy and *S*-glass/epoxy. It was shown that significant improvement in the overall stability level can be attained as compared with a baseline shell design. In fact, the developed methodology has been proved to be a useful design tool for selecting an optimal stacking sequence of a thin-walled anisotropic ring/long cylinder having arbitrary thickness-to-radius ratio.

1. Introduction

Many mechanical and structural elements made of fiber reinforced composites are increasingly utilized in aerospace, marine and civil engineering applications [Vinson 1992; Daniel and Ishai 2006]. The most important benefits from using such advanced materials in the various structural types are the attainment of high stiffness-to-weight ratio and long fatigue life. One common application is the design of composite cylindrical shells under the action of external hydrostatic pressure, which might cause collapse by buckling instability [Simitses 1996; Sridharan and Kasagi 1997]. Examples are the underground and underwater pipelines, rocket motor casing, boiler tubes subjected to external steam pressure, and reinforced submarine structures. The composite cylindrical vessels for underwater applications [Davies and Chauchot 1999] are intended to operate at high external hydrostatic pressure (sometimes up to 60 MPa). For deep-submersible long-unstiffened vessels, the hulls are generally realized using multilayered, cross-ply, composite cylinders obtained following the filament winding process [Graham 1995]. On the other hand, previous numerical and experimental studies have shown that failure due to

Keywords: buckling instability, structural optimization, fibrous composite, laminated ring/cylindrical shell, external hydrostatic pressure.

structural buckling is also a major risk factor for thin laminated cylindrical shells. Anastasiadis and Simitses [1993] studied the buckling of long laminated cylindrical shells under external radial pressure using higher order deformation theory. Their formulation, however, was restricted to symmetric lay-ups with respect to the mid-surface, to eliminate the coupling terms, as well as constant-directional pressure. More conservative results for a true fluid pressure were given by Rasheed and Yousif [2001; 2005] who applied standard energy formulation to derive the kinematics and equilibrium equations and the classical lamination theory to express the needed constitutive equations. They developed a powerful generalized closed form analytical formula for calculating stability limits of thin anisotropic rings/long cylinders subject to hydrostatic pressure. Another refined treatment of the inplane buckling of rings was given by Hodges [1999] and Hodges and Harursampath [2002]. Formulation was based on a nonlinear theory for stretching and bending of anisotropic beams having constant initial curvature in their plane of symmetry with the only restriction of small strain in the prebuckling state.

Considering next structural optimization, several papers appeared on the topic of buckling and stability optimization. Maalawi [2002] presented a piecewise structural model for buckling optimization of elastic columns under mass equality constraint. He showed that the most effective design variables that have a bearing on buckling optimization are the cross sectional area, radius of gyration and length of each segment composing the column. Another work by Maalawi and El Chazly [2002] dealt with both stability and dynamic optimization of multielement beam type structures. They formulated the associated optimization problems in a standard mathematical programming solved by the interior penalty function technique. More recently, Librescu and Maalawi [2007] considered optimization of aeroelastic stability of composite wings. They applied the concept of material grading with the implementation of both continuous and piecewise structural models. For fibrous laminated composite structures, the optimization of ply angles and thicknesses could allow the properties of the laminate to be tailored to a specific application. ZitzEvancih [1985] applied NASA buckling equations for the optimization of orthotropic cylinders against buckling. Balanced symmetric plies, consisting of $0°$, $\pm 45°$ and $90°$ fiber orientations, were used to construct the laminates. The relative volume ratio of the laminates to each other and the stacking sequence were used as the optimization design variables. Chattopadhyay and Ferreira [1993] performed a study to investigate the maximum buckling load of a cylinder subject to ply stress constraints using material and geometric design variables. A closed form shell equation was utilized for the buckling load calculation. Laminates were constrained to be symmetric, and the number of plies was included in the design variables. Results for graphite/epoxy, glass/epoxy and Kevlar/epoxy models were found using the computer code CONMIN. Considering optimization of underwater cylindrical vessels, Tanguy et al. [2002] dealt with the optimal design of deep submarine vehicles. They developed a genetic algorithm procedure coupled with an analytical model to determine the laminate stacking sequences that maximize the critical external buckling pressure. They also showed that the measured buckling pressures for glass/epoxy and carbon/epoxy cylinders appear to be in good agreement with numerical results and demonstrated the gains due to the optimized laminations.

The aim of the present study is to achieve enhanced stability limits of anisotropic ring/long cylindrical shell structures subjected to hydrostatic external pressure. Based on the analytical buckling model developed by Rasheed and Yousif [2005], a useful optimization tool has been built for designing efficient configurations with improved buckling stability. This allows the search for the stacking sequences that maximize the buckling pressure and at the same time takes into account the manufacturing requirements. The

corresponding increases in the buckling pressures calculated with respect to a baseline design have been evaluated for several configurations, including cases of orthotropic, filament wound rings/long cylinders fabricated from three different types of composite materials, namely E-glass/vinyl-ester, graphite/epoxy and S-glass/epoxy. It is assumed that the volume fractions of the constituent materials of the composite structure remain constant during optimization, so that the total structural mass is held at its reference value corresponding to the baseline design. The final results demonstrated the usefulness of the given methodology in attaining substantial improvement in the overall stability level of thin-walled anisotropic rings/long cylinders having arbitrary thickness-radius ratio, which is a major contribution of this paper.

2. Structural analysis

In this section, the basic structural analysis of multiangle laminated composite lay-ups that are widely used in filament wound rings/long cylinders are considered. In order to restrict the time of calculation to acceptable values for the developed optimization tool, the analytical formulation shall be based on the derivation in two fruitful papers by Rasheed and Yousif [2001; 2005], which are based on the assumption of small hoop strain and rotation of circumferential elements. Such an approach provides good sensitivity to lamination parameters, and allows the search for the needed optimal stacking sequences, which maximize the buckling pressure in a reasonable computational time.

Following the standard procedures of the classical lamination theory [Soden et al. 1998; Reddy 2004], the matrix equation, which relates the resultant, distributed forces (N_{xx}, N_{ss}, N_{xs}) and moments (M_{xx}, M_{ss}, M_{xs}) to the strains $(\varepsilon^0_{xx}, \varepsilon^0_{ss}, \gamma^0_{xa})$ and curvatures $(\kappa_{xx}, \kappa_{ss}, \kappa_{xs})$ at the middle surface of the shell structure, can be written as

$$\begin{pmatrix} N_{xx} \\ N_{ss} \\ N_{xs} \\ M_{xx} \\ M_{ss} \\ M_{xs} \end{pmatrix} = \begin{pmatrix} A_{11} & A_{12} & A_{16} & B_{11} & B_{12} & B_{16} \\ A_{12} & A_{22} & A_{26} & B_{12} & B_{22} & B_{26} \\ A_{16} & A_{26} & A_{66} & B_{16} & B_{26} & B_{66} \\ B_{11} & B_{12} & B_{16} & D_{11} & D_{12} & D_{16} \\ B_{12} & B_{22} & B_{26} & D_{12} & D_{22} & D_{26} \\ B_{16} & B_{26} & B_{66} & D_{16} & D_{26} & D_{66} \end{pmatrix} \begin{pmatrix} \varepsilon^0_{xx} \\ \varepsilon^0_{ss} \\ \gamma^0_{xs} \\ \kappa_{xx} \\ \kappa_{ss} \\ \kappa_{xs} \end{pmatrix}, \tag{1}$$

where (x, s, z) are the axial, tangential and radial coordinates, respectively, and the matrix elements (A_{ij}, B_{ij}, D_{ij}) are called the extensional, coupling and bending stiffness coefficients, respectively. They are all defined in Appendix A, along with the necessary kinematical relations and constitutive equations utilized in deriving (1). Actually, the kinematical relations follow the same expressions derived for thin isotropic rings [Brush and Almroth 1975; Simitses 1976]. Both cases of laminated composite rings and long cylindrical shells are considered. It was shown by Rasheed and Yousif [2005] that the only significant strain components in both cases are the hoop strain ε^0_{ss} and the circumferential curvature κ_{ss} of the mid-surface; see Appendix A. The reduced form of (1) for the two cases was shown to be

$$\begin{pmatrix} N_{ss} \\ M_{ss} \end{pmatrix} = \begin{pmatrix} A_{\text{ani}} & B_{\text{ani}} \\ B_{\text{ani}} & D_{\text{ani}} \end{pmatrix} \begin{pmatrix} \varepsilon^0_{ss} \\ \kappa_{ss} \end{pmatrix}. \tag{2}$$

In the case of thin rings the axial and shear forces (N_{xx}, N_{xs}) must vanish along the free edges. The bending and twisting moments (M_{xx}, M_{xs}) may also be neglected. Therefore, the first, third, fourth and

sixth rows of (1) are solved for the strains and curvatures in terms of $(\varepsilon^0_{ss}, \kappa_{ss})$ to give the following matrix relation

$$S_1 \begin{pmatrix} \varepsilon^0_{xx} \\ \gamma^0_{xs} \\ \kappa_{xx} \\ \kappa_{xs} \end{pmatrix} = -S_2 \begin{pmatrix} \varepsilon^0_{ss} \\ \kappa_{ss} \end{pmatrix},$$

or

$$\begin{pmatrix} \varepsilon^0_{xx} \\ \gamma^0_{xs} \\ \kappa_{xx} \\ \kappa_{xs} \end{pmatrix} = -S_1^{-1} S_2 \begin{pmatrix} \varepsilon^0_{ss} \\ \kappa_{ss} \end{pmatrix}, \tag{3}$$

where

$$S_1 = \begin{pmatrix} A_{11} & A_{16} & B_{11} & B_{16} \\ A_{16} & A_{66} & B_{16} & B_{66} \\ B_{11} & B_{16} & D_{11} & D_{16} \\ B_{16} & B_{66} & D_{16} & D_{66} \end{pmatrix}, \quad \text{and} \quad S_2 = \begin{pmatrix} A_{12} & B_{12} \\ A_{26} & B_{26} \\ B_{12} & D_{12} \\ B_{26} & D_{26} \end{pmatrix}.$$

Substituting (3) back into (1), we can show that

$$\begin{pmatrix} A_{\text{ani}} & B_{\text{ani}} \\ B_{\text{ani}} & D_{\text{ani}} \end{pmatrix}_{\text{ring}} = \begin{pmatrix} A_{22} & B_{22} \\ B_{22} & D_{22} \end{pmatrix} - S_2^T S_1^{-1} S_2. \tag{4}$$

For the case of a long cylinder, the out-of-plane displacements are restrained, that is,

$$\varepsilon^0_{xx} = \gamma^0_{xs} = \kappa_{xs} = 0.$$

Therefore, the only strains to be taken into considerations are the in-plane hoop strain ε^0_{ss} and the circumferential curvature κ_{ss}. Accordingly, the reduced matrix of (2) takes the following form

$$\begin{pmatrix} A_{\text{ani}} & B_{\text{ani}} \\ B_{\text{ani}} & D_{\text{ani}} \end{pmatrix}_{\text{cylinder}} = \begin{pmatrix} A_{22} & B_{22} \\ B_{22} & D_{22} \end{pmatrix}. \tag{5}$$

3. Analytical buckling model

The governing differential equations of anisotropic rings/long cylinders subjected to external pressure are similar to those of the isotropic case [Brush and Almroth 1975; Simitses 1976].

They are cast in the following:

$$\begin{aligned} M'_{ss} + R(N'_{ss} - \beta N_{ss}) &= \beta p R^2, \\ M''_{ss} - R\big(N_{ss} + (\beta N_{ss})' + p(w_0 + v'_0)\big) &= pR^2, \end{aligned} \tag{6}$$

where the prime denotes differentiation with respect to angular position φ, and

$$\beta = \frac{1}{R}(v_0 - w'_0).$$

Definitions of other parameters are given in Appendix A. Rasheed and Yousif [2001; 2005] presented two solutions for (6): one for the prebuckled state and the other termed as the bifurcation solution obtained

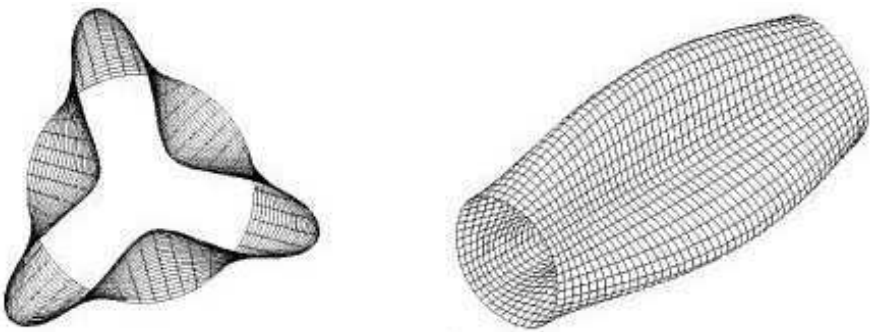

Figure 1. Characteristic buckling mode of a laminated long cylinder [Simitses 1996].

by perturbing the displacements about the prebuckling solution. They finally arrived at a closed form solution for the critical buckling pressure given by

$$p_{cr} = 3\frac{D_{\text{ani}}}{R^3}\left(\frac{1-\frac{\psi^2}{\alpha}}{1+\alpha+2\psi}\right), \quad \psi = \frac{1}{R}\frac{B_{\text{ani}}}{A_{\text{ani}}}, \quad \alpha = \frac{1}{R^2}\frac{D_{\text{ani}}}{A_{\text{ani}}}, \tag{7}$$

where the stiffness coefficients A_{ani}, B_{ani} and D_{ani} can be calculated from (4) for the case of circular rings and from (5) for long cylinders. It is to be noticed here that the formula given in (7) for calculating p_{cr} is only valid for thin rings/cylinders with thickness-to-radius ratio $h/R \leq 0.1$ [Rasheed and Yousif 2001]. A typical buckling mode of laminated long cylinder is shown in Figure 1.

The reduced forms of (7) for some limiting cases where $\psi = 0$ and $\alpha \ll 1$ are given in Table 1.

4. Optimization problem statement

The associated optimization problem shall seek maximization of the external hydrostatic pressure p_{cr} at which buckling instability might occur. Optimization variables include the total number of plies n,

Limiting Cases	Critical buckling pressure $p_{cr} = 3D/R^3$ Bending stiffness, D
Thin isotropic rings [Brush and Almroth 1975].	$Eh^3/12$
Thin isotropic long cylinders [Simitses 1976].	$Eh^3/12(1-\nu^2)$
Thin orthotropic rings [Anastasiadis and Simitses 1993]	$E_{22}h^3/12$
Thin orthotropic long cylindrical shells with fibers parallel to the shell axis x [Anastasiadis and Simitses 1993]	$E_{22}h^3/12(1-\nu_{12}\nu_{21})$

Table 1. Buckling pressure formulas for limiting cases $\psi = 0$ and $\alpha \ll 1$. E, ν = isotropic modulus of elasticity and Poisson's ratio, E_{22} = hoop modulus, ν_{12} = Poisson's ratio for axial load, $\nu_{21} = \nu_{12}E_{22}/E_{11}$ (in cases with fibers perpendicular to the shell axis, E_{22} should be replaced by E_{11})

.

thickness h_k and fiber orientation angle θ_k of the individual k-th ply. Side constraints are always imposed on the design variables for geometrical, manufacturing or logical reasons to avoid having unrealistic odd shaped optimum designs.

4A. ***Definition of the baseline design.*** It is convenient first to normalize all variables and parameters with respect to a baseline design, which has been selected to be a unidirectional orthotropic laminated ring/long cylinder with the fibers parallel to the shell axis x. Optimized shell designs shall have the same material properties, mean radius R and total shell thickness h of the baseline design. Therefore, the preassigned parameters, which are not subject to change in the optimization process, ought to be the type of material of construction, mean radius and total thickness of the shell.

Using the formulas given in Table 1 for cases of orthotropic shells, we define expressions for calculating the critical buckling pressure P_{cro} of the baseline design in Table 2, which depend upon the type of composite material utilized and the shell thickness-to-radius ratio h/R as well.

4B. ***Proposed optimization model.*** The search for the optimized lamination can be performed by coupling the analytical buckling shell model to a standard nonlinear mathematical programming procedure. The design variable vector $\underline{X}_d$, which is subject to change in the optimization process, is defined as $\underline{X}_d = (\hat{h}_k, \theta_k)_{k=1,2,\ldots,n}$, where the dimensionless thickness of the k-th lamina is defined by $\hat{h}_k = h_k/h$. Therefore, the buckling optimization problem considered herein may be cast in the following standard mathematical programming form:

$$\begin{aligned} &\text{Maximize} && \hat{p}_{cr} \\ &\text{subject to} && h_L \le \hat{h}_k \le h_U, \\ & && \theta_L \le \theta_k \le \theta_U \quad k = 1, 2, \ldots, n \\ & && \sum_{k=1}^{n} \hat{h}_k = 1, \end{aligned}$$

where $\hat{p}_{cr} = p_{cr}/p_{\text{cro}}$ is the dimensionless critical buckling pressure and h_L, h_U are the lower and upper bounds imposed on the individual dimensionless ply thicknesses. According to the filament-winding manufacturing process, each ply is characterized by its filament-winding angle θ_k with respect to the

	Orthotropic mechanical properties* (GPa)				$p_{\text{cro}}x(h/R)^3$ (GPa)	
Material Type	E_{11}	E_{22}	G_{12}	ν_{12}	Rings	Cylinders
E-glass/vinyl-ester	41.06	6.73	2.5	0.299	1.683	1.708
graphite/epoxy	130.0	7.0	6.0	0.28	1.75	1.757
S-glass/epoxy	57.0	14.0	5.7	0.277	3.50	3.567

Table 2. Material properties and critical buckling pressure of the baseline design (p_{cro}).
*Taken from [Rasheed and Yousif 2001].

cylinder axis x. The stacking sequence is denoted by $[\theta_1/\theta_2/\cdots/\theta_n]$, where the angles are given in degrees, starting from the outer surface of the shell. In addition, in a real-world manufacturing process, the filament-winding angles θ_k must be chosen from a limited range of allowable lower (θ_L) and upper (θ_U) values according to technology references. It is important to mention here that the volume fractions of the constituent materials of the composite structure are assumed not to significantly change during optimization, so that the total structural mass remains constant at its reference value of the baseline design. The effect of changing the volume fractions is now under study by the author, where the concept of material grading will be considered [Librescu and Maalawi 2007].

This optimization problem may be thought as a search in a $2n$-dimensional space for a point corresponding to the maximum value of the objective function such that it lies within the region bounded by subspaces representing the constraint functions [Vanderplaats 1994; Venkataraman 2002]. The usefulness and efficiency of penalty methods (see Appendix B) for solving this kind of optimization problems have been explored intensively in the literature [Maalawi and El Chazly 2002]. The constraints are taken into account indirectly by transforming the constrained problem into a series of unconstrained problems. Several software packages are available now for solving mathematical programming problems. The MATLAB optimization toolbox [Venkataraman 2002] offers routines that implement the interior penalty function method, which has a wide applicability in many engineering applications, via a built-in function named "fminsearch".

5. Results and discussions

The given approach discussed in previous sections shall be applied here to several cases of study of thin-walled anisotropic rings/long cylinders subjected to external hydrostatic pressure. The materials of construction are chosen to be E-glass/vinyl-ester, graphite/epoxy and S-glass/epoxy. The functional behavior of the candidate objective function, as represented by maximization of the dimensionless buckling pressure $\hat{p}_{cr}$, is thoroughly investigated in order to see how it is changed with the optimization variables in the selected design space. The final optimum designs recommended by the model will directly depend on the mathematical form and behavior of the objective function.

5A. ***Two-layer anisotropic long cylinder.*** The first case study to be considered herein is a long thin-walled cylindrical shell fabricated from E-glass/vinyl-ester composites with the lay-up composed of only two plies ($n = 2$) having equal thicknesses ($\hat{h}_1 = \hat{h}_2 = 0.5$) and different fiber orientation angles. Figure 2 shows the developed level curves of the dimensionless buckling pressure $\hat{p}_{cr}$ (also named isomerits or isobars) in the θ_1-θ_2 design space. It is seen that the objective function is well behaved in the selected design space with a symmetrical-shaped contours about the two lines $\theta_1 = 0$ and $\theta_2 = 0$ corresponding to the baseline design in which $\hat{p}_{cr} = 1.0$, representing a point of global minima.

With the special case of $\pm 63^\circ$ angle-ply E-glass/vinyl-ester cylinder, the present model gives $\hat{p}_{cr} = 4.23$, that is, $p_{cr} = 4.23 \times 1.708 \times (h/R)^3$ GPa, depending on the shell thickness-to-radius ratio (refer to Table 2). The actual dimensional values of the critical buckling pressure for the different thickness ratios have been calculated from just one point in the design space of Figure 2: a significant contribution and gain from the given optimization formulation. The corresponding values are given in Table 3 for the cases of baseline design, helically wound [$\pm 63^\circ$] and [$\pm 90^\circ$] hoop layers. It is seen that the results compare very well with those given by Rasheed and Yousif [2001]. The unconstrained maximum value

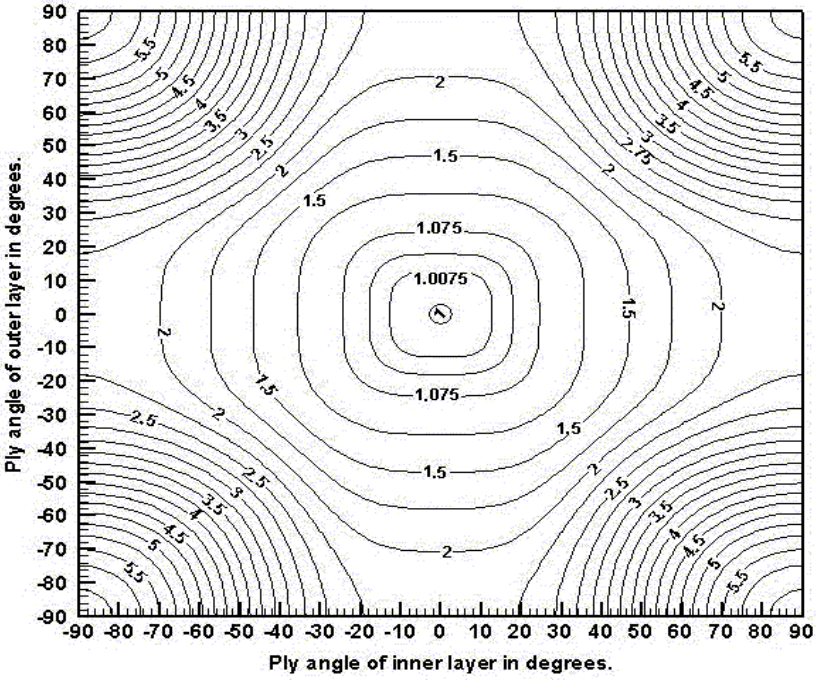

Figure 2. Dimensionless buckling pressure $\hat{p}_{cr}$ in the $[\theta_1/\theta_2]$ design space. Two-ply cylinder made of E-glass/vinyl-ester ($\hat{h}_1 = \hat{h}_2 = 0.5$).

of the critical buckling pressure occurs at any one of the corners of Figure 2 corresponding to the four design points $[\theta_1/\theta_2] = [\pm 90^\circ / \pm 90^\circ]$ where $\hat{p}_{cr} = 6.1$.

To examine the effect of using another type of constructional material, we show in Figure 3 the developed isomerits for a two-ply long cylinder fabricated from graphite/epoxy composites. As seen the shape of the level curves is similar to that of Figure 2, but with higher stability levels, reaching a maximum value of $\hat{p}_{cr} = 18.57$ for a hoop wound construction.

Table 4 presents the solutions for the $[\pm 45^\circ]$ angle-ply and the $[90^\circ]$ cross-ply constructions for different thickness-to-radius ratios. Results are compared with those in [Rasheed and Yousif 2001], which

h/R	Baseline $[0^\circ]$ $\hat{p}_{cr} = 1.00$	Helically wound $[\pm 63^\circ]$ 4.23	Hoop plies $[\pm 90^\circ]$ 6.10
1/15	506.07	2140.69	3087.05
1/20	213.50	903.11	1302.35
1/25	109.31	462.39	666.80
1/50	13.66	57.80	83.35

Table 3. Critical buckling pressure for E-glass/vinyl-easter cylinders with different layups ($p_{cr} = \hat{p}_{cr} \times 1.708(h/R)^3$ GPa).

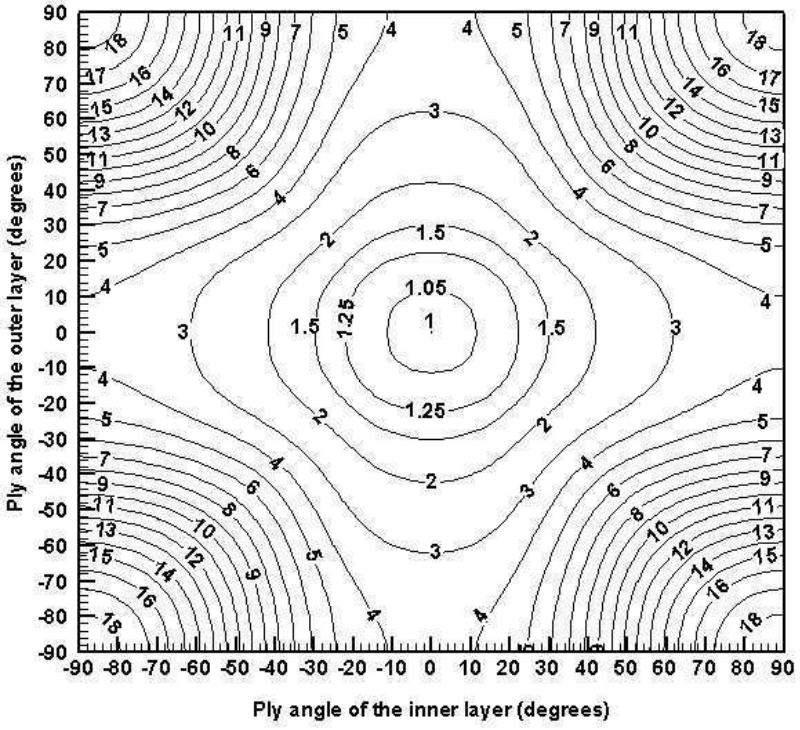

Figure 3. $\hat{p}_{cr}$-isomerits for a graphite/epoxy, two-layer cylinder in $[\theta_1/\theta_2]$ design space $(\hat{h}_1 = \hat{h}_2 = 0.5)$.

were based on the assumption that adjacent $[\pm\theta]$ layers are merged together with the stiffness coefficients taken as average values from the $(+\theta)$ and $(-\theta)$ plies. These solutions are also valid for lay-ups $[0_3^\circ]_s$, $[90_3^\circ]_s$, $[45_2^\circ/-45_2^\circ]_s$ and $[45^\circ/-45^\circ/45^\circ/-45^\circ]_s$, which were numbered 1, 8, 20 and 21 in the papers by Anastasiadis and Simitses [1993] and Rasheed and Yousif [2001].

The case of a helically wound lay-up construction $[+\theta/-\theta]$ with unequal play thicknesses $\hat{h}_1$ and $\hat{h}_2$, such that their sum is held fixed at a value of unity, has also been investigated. Computer solutions have shown that no significant change in the resulting values of the critical buckling pressure can be remarked in spite of the wide change in the ply thicknesses. This is a natural expected result since

	Baseline [0°]	Helically wound [±45°]	Hoop plies [±90°]
	$\hat{p}_{cr} = 1.00$	5.9	18.57
h/R			
1/15	520.59	3071.50	9667.40
1/50	14.06	82.93	261.02
1/120	1.02	5.99	18.88

Table 4. Critical buckling pressure for graphite/epoxy cylinders with different lay-ups $(p_{cr} = \hat{p}_{cr} \times 1.757(h/R)^3$ GPa).

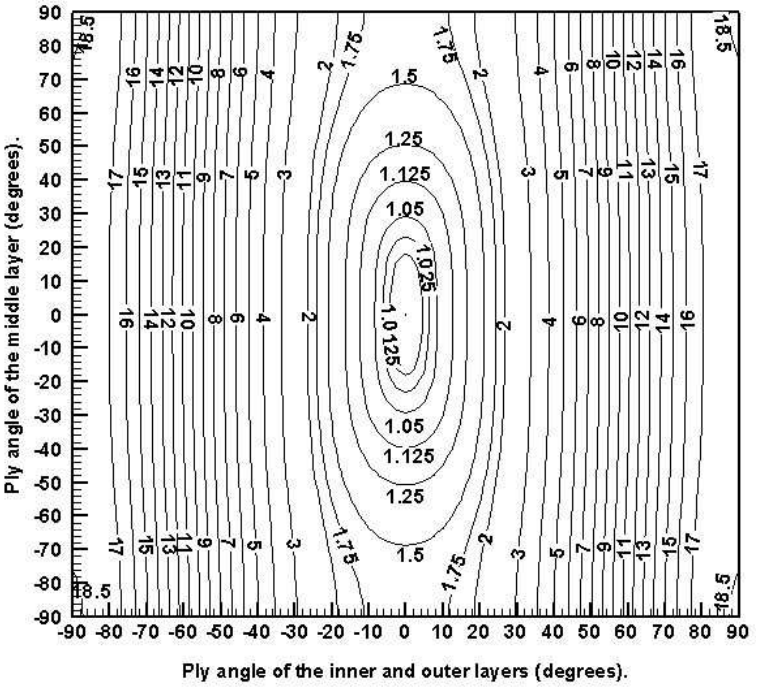

Figure 4. $\hat{p}_{cr}$- isomerits for three-ply graphite/epoxy cylinder $[\theta_1/\theta_2/\theta_1]$.

the stiffness coefficients A_{ani}, B_{ani} and D_{ani} remain unchanged for such lay-up construction. Also, it should be mentioned here that the optimal buckling pressure for a cylinder having stacking sequence $[+\theta_1/-\theta_1/+\theta_2/-\theta_2]$ is identical to that obtained before for stacking sequence $[\theta_1/\theta_2]$, as given in Figures 2 and 3.

5B. ***Three-layer anisotropic long cylinder.*** Figure 4 shows the developed isomerits for a cylinder constructed from three equally-thicked layers with stacking sequence denoted by $[\theta_1/\theta_2/\theta_1]$. The same behavior can be observed as before, but with slight flattening in the θ_2-direction. The contours are fully symmetrical about the mid-point corresponding to the minimal baseline value of unity. Two distinct zones can be seen: the closed middle one containing the global minima, and the open one covering the two ranges $\theta_1 < -30^\circ$ and $\theta_1 > 30^\circ$ in which the critical buckling pressure is not much affected by variation in the ply angle θ_2.

Other computational results for cross-ply lamination are given in Table 5, where substantial increase in the critical bucking pressure by changing the ply angles can be observed. Similar solutions were obtained for the stacking sequences $[0_2^\circ/90^\circ]_s$ and $[90_2^\circ/0^\circ]_s$, which corresponds to lay-up numbers 2 and 7 considered by Anastasiadis and Simitses [1993].

5C. ***Four-layer sandwiched anisotropic cylinder.*** The same graphite/epoxy cylinder is reconsidered here with changing the stacking sequence to become $\pm 20^\circ$ equal-thickness layers sandwiched in between outer and inner 90° hoop layers with unequal thicknesses $\hat{h}_2 = \hat{h}_3$, $\hat{h}_1 \neq \hat{h}_4$, such that the thickness equality

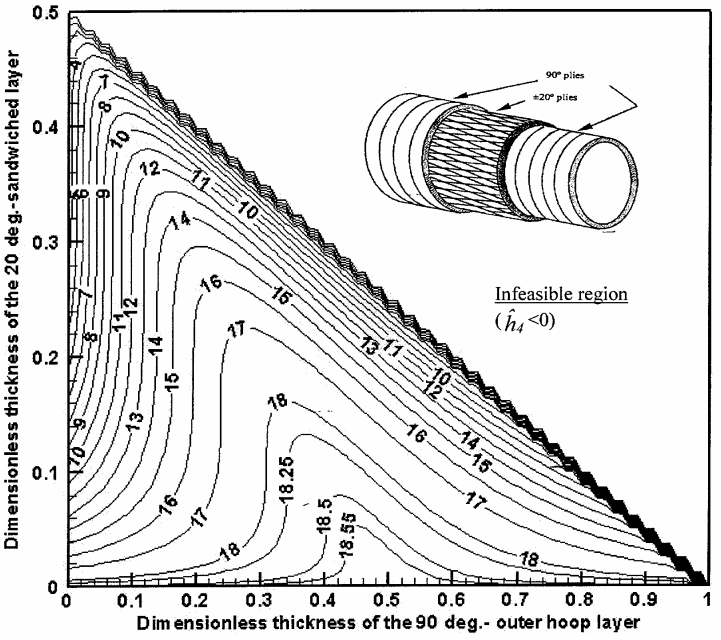

Figure 5. Design space for a sandwich lay-up graphite/epoxy cylinder $[90°/\pm 20°/90°]$.

constraint

$$\sum_{k=1}^{4} \hat{h}_k = 1$$

is always satisfied. Figure 5 shows the developed $\hat{p}_{cr}$-isomerits in the $\hat{h}_1$-$\hat{h}_2$ design space. The contours inside the feasible domain, which is bounded by the three lines $\hat{h}_1 = 0$, $\hat{h}_2 = 0$ and $\hat{h}_1 + 2\hat{h}_2 = 1$ (that is, $\hat{h}_4 = 0$), are obliged to turn sharply to be asymptotes to the line $\hat{h}_4 = 0$, in order not to violate the thickness equality constraint. This is why they appear in the figure as zigzagged lines.

It is clear now that all tabulated results given by Rasheed and Yousif [2001] can be directly obtained from just one design point in Figure 5, namely $(\hat{h}_1, \hat{h}_2) = (0.25, 0.25)$ at which $\hat{p}_{cr} = 16.43$ (see Table 6). As a general observation, as the thickness of the hoop layers increase, a substantial increase in the critical

h/R	Baseline $[0_3^\circ]$ $\hat{p}_{cr} = 1.00$	$[0°/90°/0°]$ 1.651	$[90°/0°/90°]$ 17.92
1/15	520.59	859.57	9331.19
1/50	14.06	23.21	251.94
1/120	1.02	1.68	18.23

Table 5. Critical buckling pressure for graphite/epoxy cylinders $[\theta_1/\theta_2/\theta_1]$ ($p_{cr} = \hat{p}_{cr} \times 1.757(h/R)^3$ GPa).

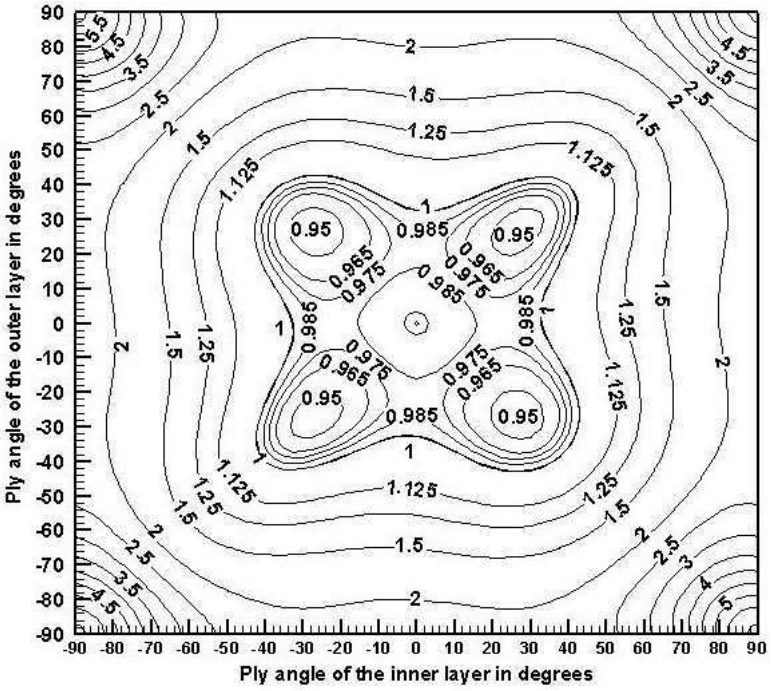

Figure 6. Butterfly-like zone containing the local minimal stability limits in $[\theta_1/\theta_2]$ design space for two-layer, E-glass/vinyl-easter ring ($\hat{h}_1 = \hat{h}_2 = 0.5$).

buckling pressure will be achieved; for example, at $(\hat{h}_1, \hat{h}_2) = (0.33, 0.17)$, $\hat{p}_{cr} = 17.92$ representing a percentage increase of $(17.92 - 16.43)/16.43 = 9.1\%$.

5D. ***Anisotropic thin rings.*** In this section, some study cases of thin rings will be examined to see the effect of anisotropy for different angle-ply stacking sequences. The first example considers a ring fabricated from E-glass/vinyl-ester having two equal-thickness layers with stacking $[\theta_1/\theta_2]$. Figure 6 shows the developed $\hat{p}_{cr}$-isomerits, which are symmetrical about the two lines $\theta_1 = 0$ and $\theta_2 = 0$ corresponding to the baseline value of unity. The region in the middle resembles a butterfly containing four local minima $[\pm 30^\circ/\pm 30^\circ]$, where $\hat{p}_{cr} = 0.94$ representing about 6% degradation in the stability level. The butterfly bounding contour determines stacking sequences having buckling pressure equals to that of the baseline design (namely, $\hat{p}_{cr} = 1$). The unconstrained global maximum value of the critical buckling pressure occurs at any one of the four design points $[\theta_1/\theta_2] = [\pm 90^\circ/\pm 90^\circ]$ where $\hat{p}_{cr} = 6.1$. The constrained

h/R	1/15	1/20	1/25	1/50
p_{cr} (GPa)	8553.0	3609.3	1847.5	231.0

Table 6. Critical buckling pressure for graphite/epoxy cylinders $[90^\circ/\pm 20^\circ/90^\circ]$ ($\hat{p}_{cr} = 16.43$, $p_{\text{cro}} = 1.757(h/R)^3$ GPa, $p_{cr} = \hat{p}_{cr} \cdot p_{\text{cro}}$).

h/R	$[+63°]$ $\hat{p}_{cr} = 1.754$	$[+63°/-63°]$ 2.166	$[+63°/-63°]_3$ 3.134	$[+63°/-63°]_\infty$ 3.234
1/20	369.00	455.67	659.32	680.35
1/50	23.62	29.16	42.20	43.54
1/100	2.95	3.65	5.27	5.44

Table 7. Critical buckling pressure for E-glass/vinyl-easter thin rings ($p_{cr} = \hat{p}_{cr} \times 1.683(h/R)^3$ GPa).

solutions for the special case of $\pm 63°$ angle-ply, which was considered by Rasheed and Yousif [2005], are summarized in Table 7, including also the extreme cases of full anisotropy represented by the lay-up with only $[+63°]$ plies for the entire thickness and the fully orthotropic lamination consisting of many too thin alternating balanced plies $[+63°/-63°]$, which produce the highest possible buckling capacity.

A last example considers a thin ring fabricated from S-glass/epoxy with the mechanical properties given in Table 2. The lay-up consists of three $[+45°/-45°]$ balanced plies, each with equal thickness, that is, $[h_k/h_k]_{k=1,2,3}$ where h_k is the thickness of a single lamina. Figure 7 depicts the developed $\hat{p}_{cr}$-isomerits in the $\hat{h}_1$-$\hat{h}_2$ design space. As seen, the feasible domain is bounded by the three straight lines $\hat{h}_1 = 0$, $\hat{h}_2 = 0$ and $\hat{h}_1 + \hat{h}_2 = 0.5$, where an infinite number of level curves are obliged to turn to be tangent to the latter one in order not to violate the thickness equality constraint. The global optimal solution has shown to be of equal ply thickness: $\hat{h}_k = 0.167$, $k = 1, 2, 3$, where $\hat{p}_{cr} = 1.2593$. The calculated dimensional value of the maximum buckling pressure is given in Table 8 for different thickness to radius ratios.

6. Conclusions

In this paper, a practical approach for enhancing the buckling stability limits of thin-walled anisotropic rings/long cylinders has been developed. The formulation of an optimal lamination design against buckling has been thoroughly investigated, where useful design charts are given for several types of anisotropic rings/long cylinders showing the functional dependence of the critical buckling pressure on the stacking sequence and ply thickness as well. An analytical buckling model has been implemented, which provides good sensitivity to lamination parameters, allowing the search for the needed optimal stacking sequences in an acceptable computational time. The proposed model deals with dimensionless quantities in order to be applicable for handling thin shells having arbitrary thickness-to-radius ratios, which is a major contribution of this work. Results have indicated that the optimized laminations induce significant increases, always exceeding several tens of percent, of the buckling pressures with respect to the reference

h/R	1/15	1/20	1/25	1/50	1/100
p_{cr} (KPa)	1305.94	550.94	282.1	35.26	4.41

Table 8. Maximum buckling pressure for S-glass/epoxy rings $[+45°/-45°]_3$ ($\hat{p}_{cr} = 1.2593$, $p_{\text{cro}} = 3.5(h/R)^3$ GPa, $p_{cr} = \hat{p}_{cr} \cdot p_{\text{cro}}$).

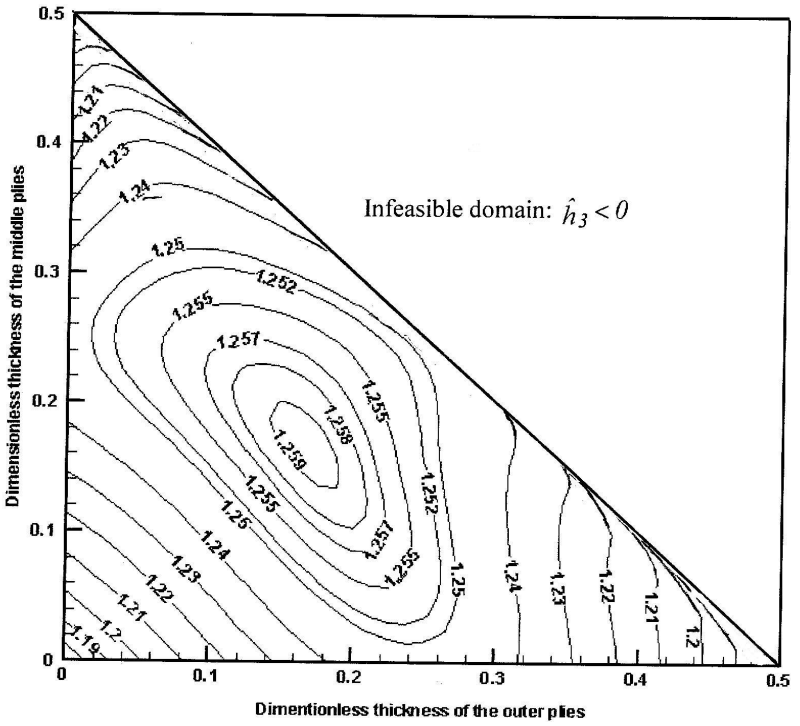

Figure 7. Global optimal stability limit in $\hat{h}_1$-$\hat{h}_2$ design space for a six-layer, S-glass/epoxy ring with a stacking sequence $[+45°/-45°]_3$.

or baseline design. It is assumed that the volume fractions of the composite material constituents do not significantly change during optimization, so that the total structural mass remains constant. Three types of composites were considered: E-glass/vinyl-ester, graphite/epoxy and S-glass/epoxy. It has been shown that the overall stability level of the laminated composite shell structures under considerations can be substantially improved by finding the optimal stacking sequence without violating any imposed side constraints. The stability limits of the optimized shells have been substantially enhanced as compared with those of the reference or baseline designs. The case of cylinders of finite length as well as the use of material grading concept for maximizing buckling stability boundaries under equality mass constraint shall be considered in the future.

Appendix A

Based upon the classical lamination theory [Reddy 2004], this appendix includes a brief derivation of the laminate stiffness parameters, which allows for a general stacking sequence optimization.

Constitutive relations. One difference between laminated composites and traditional engineering materials is that a composite response to loads is direction dependent. In order to analyze the response of a composite, we must be able to predict the behavior of individual unidirectional lamina, which is characterized by having all fibers oriented in the same direction. This model allows one to treat the lamina as an orthotropic material. In reality fibers are not perfectly straight or uniformly oriented within

the lamina. There are generally several layers of fibers nested within a single lamina. The structural model used to represent the composite laminate is schematically shown in Figure A-1.

1, 2 and 3 are denoted the principal directions of an orthotropic lamina, defined as follows:

- Direction 1: principal fiber direction, also called fiber longitudinal direction,
- Direction 2: in-plane direction perpendicular to fibers, transversal direction, and
- Direction 3: out-of-plane direction perpendicular to fibers, normal direction.

The reduced form of Hooke's law for an orthotropic homogeneous lamina in a plane stress state may be written as

$$\begin{pmatrix} \sigma_{11} \\ \sigma_{22} \\ \tau_{12} \end{pmatrix} = \begin{pmatrix} Q_{11} & Q_{12} & 0 \\ Q_{12} & Q_{22} & 0 \\ 0 & 0 & Q_{66} \end{pmatrix} \begin{pmatrix} \varepsilon_{11} \\ \varepsilon_{22} \\ \gamma_{12} \end{pmatrix}, \tag{A.1}$$

where Q is referred to as the reduced stiffeners matrix of the k-th lamina, defined in terms of material properties:

$$Q_{11} = \frac{E_{11}}{1 - \nu_{12}\nu_{21}}, \qquad Q_{22} = \frac{E_{22}}{1 - \nu_{12}\nu_{21}}, \qquad Q_{12} = \frac{\nu_{12}E_{22}}{1 - \nu_{12}\nu_{21}}, \qquad Q_{66} = G_{12},$$

where $\nu_{12}E_{22} = \nu_{21}E_{11}$.

As seen from the above equations, there are four independent elastic constants: the Young's moduli in the 1 and 2 directions, E_{11} and E_{22}, the shear modulus, G_{12}, and the major Poisson's ratio, ν_{12}, upon which the stiffness matrix of a homogeneous orthotropic composite material is calculated.

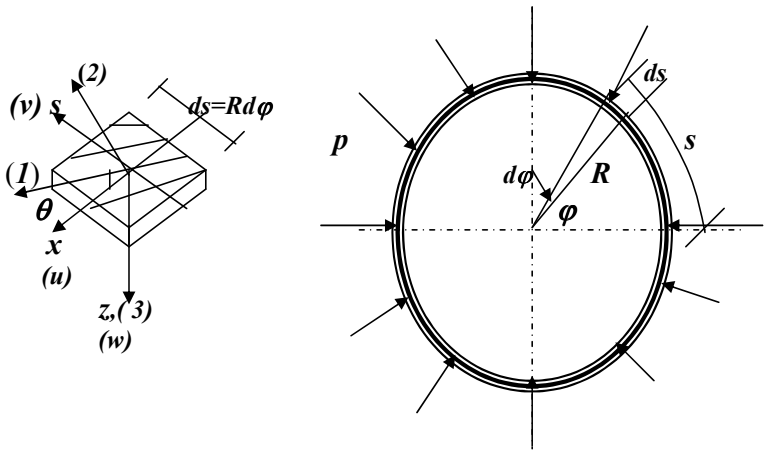

Figure A-1. Laminated composite ring/cylindrical shell under external pressure (u displacement in the axial direction x, v in the tangential direction s, w in the radial direction z).

For a generally orthotropic material, (A.1) must be transformed to reflect rotated fiber orientation angles. The following matrix relation reflects this transformation [Daniel and Ishai 2006]:

$$\begin{pmatrix}\sigma_{xx}\\ \sigma_{ss}\\ \tau_{xs}\end{pmatrix}=\begin{pmatrix}\overline{Q}_{11} & \overline{Q}_{12} & \overline{Q}_{16}\\ \overline{Q}_{12} & \overline{Q}_{22} & \overline{Q}_{26}\\ \overline{Q}_{16} & \overline{Q}_{26} & \overline{Q}_{66}\end{pmatrix}\begin{pmatrix}\varepsilon_{xx}\\ \varepsilon_{ss}\\ \gamma_{xs}\end{pmatrix}. \tag{A.2}$$

The elements of the k-th lamina stiffness matrix $\overline{Q}$, which is now referred to the reference axes of the cylindrical shell (x, s, z), are given by

$$\begin{aligned}&\overline{Q}_{11}=U_1+U_2\cos 2\theta+U_3\cos 4\theta, && \overline{Q}_{22}=U_1-U_2\cos 2\theta+U_3\cos 4\theta,\\ &\overline{Q}_{12}=U_4-U_3\cos 4\theta, && \overline{Q}_{16}=0.5\,U_2\sin 2\theta+U_3\sin 4\theta,\\ &\overline{Q}_{26}=0.5\,U_2\sin 2\theta-U_3\sin 4\theta, && \overline{Q}_{66}=0.5\,(U_1-U_4)-U_3\cos 4\theta,\end{aligned}$$

where the invariant terms U_i are solely function of the material properties. They are defined by the following expressions [Reddy 2004]:

$$\begin{aligned}&U_1=0.125\,(3Q_{11}+3Q_{22}+2Q_{12}+4Q_{66}), && U_2=0.5\,(Q_{11}-Q_{22}),\\ &U_3=0.125\,(Q_{11}+Q_{22}-2Q_{12}-4Q_{66}), && U_4=0.125\,(Q_{11}+Q_{22}+6Q_{12}-4Q_{66}).\end{aligned}$$

For classical lamination theory, it is assumed that n layers of material are perfectly bonded together, with infinitely thin, nonshear deformable boundaries. Using Kirchoff plate theory [Simitses 1976], which assumes that the in-plane displacements vary linearly through the thickness of the laminate, the displacements of a material point distance z from the middle surface are

$$\begin{aligned}u(x,s,z)&=u_0(x,s)-z\frac{\partial w_0}{\partial x},\\ v(x,s,z)&=v_0(x,s)-z\left(\frac{\partial w_0}{\partial s}-\frac{v_0}{R}\right), \qquad \left(s\cong R\varphi,\ \frac{z}{R}\ll 1\right),\\ w(x,s,z)&=w_0(x,s),\end{aligned}$$

where $u_0(x,s)$, $v_0(x,s)$ and $w_0(x,s)$ are the displacements of a generic point (x,s) on the shell middle surface $(z=0)$ in x, s and z directions, respectively.

The strain-displacement relations in terms of the middle surface strains and shell curvatures are given in the following:

$$\begin{aligned}\varepsilon_{xx}&=\varepsilon^0_{xx}+z\kappa_{xx},\\ \varepsilon_{ss}&=\varepsilon^0_{ss}+z\kappa_{ss},\\ \gamma_{xs}&=\gamma^0_{xs}+z\kappa_{xs},\end{aligned} \qquad \text{or} \qquad \begin{pmatrix}\varepsilon_{xx}\\ \varepsilon_{ss}\\ \gamma_{xs}\end{pmatrix}=\begin{pmatrix}\varepsilon^0_{xx}\\ \varepsilon^0_{ss}\\ \gamma^0_{xs}\end{pmatrix}+z\begin{pmatrix}\kappa_{xx}\\ \kappa_{ss}\\ \kappa_{xs}\end{pmatrix}, \tag{A.3}$$

where the middle surface strains and curvatures are [Brush and Almroth 1975]

$$\varepsilon^0_{xx} = \frac{\partial u_0}{\partial x}, \qquad \kappa_{xx} = -\frac{\partial^2 w_0}{\partial x^2},$$
$$\varepsilon^0_{ss} = \frac{\partial v_0}{\partial s} + \frac{w_0}{R} + \tfrac{1}{2}\Big(\frac{\partial w_0}{\partial s} - \frac{v_0}{R}\Big)^2, \qquad \kappa_{ss} = -\frac{\partial}{\partial s}\Big(\frac{\partial w_0}{\partial s} - \frac{v_0}{R}\Big),$$
$$\gamma^0_{xs} = \frac{\partial u_0}{\partial s} + \frac{\partial v_0}{\partial x}, \qquad \kappa_{xs} = 2\frac{\partial}{\partial x}\Big(\frac{\partial w_0}{\partial s} - \frac{v_0}{R}\Big).$$

Substituting for the total strains from (A.3) into (A.2) we have

$$\begin{pmatrix}\sigma_{xx}\\ \sigma_{ss}\\ \tau_{xs}\end{pmatrix}_k = \begin{pmatrix}\overline{Q}_{11} & \overline{Q}_{12} & \overline{Q}_{16}\\ \overline{Q}_{12} & \overline{Q}_{22} & \overline{Q}_{26}\\ \overline{Q}_{16} & \overline{Q}_{26} & \overline{Q}_{66}\end{pmatrix}_k \left(\begin{pmatrix}\varepsilon^0_{xx}\\ \varepsilon^0_{ss}\\ \gamma^0_{xs}\end{pmatrix} + z\begin{pmatrix}\kappa_{xx}\\ \kappa_{ss}\\ \kappa_{xs}\end{pmatrix}\right). \tag{A.4}$$

The resultant forces and moments per unit length applied at the middle surface are defined by the integrals

$$\textit{Forces}: \qquad \begin{pmatrix}N_{xx}\\ N_{ss}\\ N_{xs}\end{pmatrix} = \int_{-h/2}^{h/2}\begin{pmatrix}\sigma_{xx}\\ \sigma_{ss}\\ \tau_{xs}\end{pmatrix} dz = \sum_{k=1}^{n}\int_{z_{k-1}}^{z_k}\begin{pmatrix}\sigma_{xx}\\ \sigma_{ss}\\ \tau_{xs}\end{pmatrix} dz, \tag{A.5}$$

$$\textit{Moments}: \qquad \begin{pmatrix}M_{xx}\\ M_{ss}\\ M_{xs}\end{pmatrix} = \int_{-h/2}^{h/2}\begin{pmatrix}\sigma_{xx}\\ \sigma_{ss}\\ \tau_{xs}\end{pmatrix} z\,dz = \sum_{k=1}^{n}\int_{z_{k-1}}^{z_k}\begin{pmatrix}\sigma_{xx}\\ \sigma_{ss}\\ \tau_{xs}\end{pmatrix} z\,dz. \tag{A.6}$$

Substituting for the stress-strain relationships of (A.4) into (A.5) and (A.6), we get

$$\begin{pmatrix}N_{xx}\\ N_{ss}\\ N_{xs}\\ M_{xx}\\ M_{ss}\\ M_{xs}\end{pmatrix} = \begin{pmatrix}A_{11} & A_{12} & A_{16} & B_{11} & B_{12} & B_{16}\\ A_{12} & A_{22} & A_{26} & B_{12} & B_{22} & B_{26}\\ A_{16} & A_{26} & A_{66} & B_{16} & B_{26} & B_{66}\\ B_{11} & B_{12} & B_{16} & D_{11} & D_{12} & D_{16}\\ B_{12} & B_{22} & B_{26} & D_{12} & D_{22} & D_{26}\\ B_{16} & B_{26} & B_{66} & D_{16} & D_{26} & D_{66}\end{pmatrix}\begin{pmatrix}\varepsilon^0_{xx}\\ \varepsilon^0_{ss}\\ \gamma^0_{xs}\\ \kappa_{xx}\\ \kappa_{ss}\\ \kappa_{xs}\end{pmatrix},$$

where A_{ij} are called the extensional stiffnesses given by $A_{ij} = \sum_{k=1}^{n} (\overline{Q}_{ij})_k (z_k - z_{k-1})$. B_{ij} are called the bending-extensional stiffnesses given by

$$B_{ij} = \tfrac{1}{2}\sum_{k=1}^{n} (\overline{Q}_{ij})_k (z_k^2 - z_{k-1}^2).$$

D_{ij} are called the bending stiffnesses

$$D_{ij} = \tfrac{1}{3}\sum_{k=1}^{n} (\overline{Q}_{ij})_k (z_k^3 - z_{k-1}^3),$$

where n is the number of different plies in the stacking sequence.

Appendix B: The interior penalty function technique

In this method the original objective function $F(\vec{x})$ is augmented with terms, called penalty terms, such that as $\vec{x}$ approaches a constraint surface one term increases indefinitely. Since the algorithm seeks to minimize the value of the objective function, it will try not to penetrate any constraint surface. Thus all constraints are taken into consideration by representing them by penalty terms in the objective function expression. The most commonly used interior penalty function [Vanderplaats 1994] is cast in the form

$$\Phi(\vec{x}, r) = F(\vec{x}) - r \sum_{j=1}^{M} \frac{1}{G_j(\vec{x})},$$

where $\Phi(\vec{x}, r)$ is the modified objective function, $G_j(\vec{x})$ is the j-th constraint function and r is a multiplier. A sequence of unconstrained minimization problems is solved with successively decreasing values of r. The MATLAB optimization toolbox [Venkataraman 2002] offers routines that implement the interior penalty function method via a built-in function named *fminsearch*.

Acknowledgment

The author wishes to thank Professor Hayder Rasheed of the Department of Civil Engineering, Kansas State University, for his valuable scientific discussions and help.

References

[Anastasiadis and Simitses 1993] J. S. Anastasiadis and G. J. Simitses, "Buckling of pressure-loaded, long, shear deformable cylindrical laminated shells", *Compos. Struct.* **23**:3 (1993), 221–231.

[Brush and Almroth 1975] D. O. Brush and B. O. Almroth, *Buckling of bars, plates and shells*, McGraw-Hill, New York, 1975.

[Chattopadhyay and Ferreira 1993] A. Chattopadhyay and J. Ferreira, "Design sensitivity and optimization of composite cylinders", *Compos. Eng.* **3** (1993), 169–179.

[Daniel and Ishai 2006] I. M. Daniel and O. Ishai, *Engineering mechanics of composite materials*, 2nd ed., Oxford University, New York, 2006.

[Davies and Chauchot 1999] P. Davies and P. Chauchot, *Composites for marine applications –Part 2: underwater structures*, Kluwer Academic, Dordrecht, 1999.

[Graham 1995] D. Graham, "Composite pressure hulls for deep ocean submersibles", *Compos. Struct.* **32**:1-4 (1995), 331–343.

[Hodges 1999] D. H. Hodges, "Non-linear inplane deformation and buckling of rings and high arches", *Int. J. Nonlinear Mech.* **34**:4 (1999), 723–737.

[Hodges and Harursampath 2002] D. H. Hodges and D. Harursampath, "Inplane buckling of anisotropic rings", in *Proceedings of the 15th ASCE Engineering Mechanics Division Conference* (New York), Columbia University, New York, June 2–5 2002.

[Librescu and Maalawi 2007] L. Librescu and K. Y. Maalawi, "Material grading for improved aeroelastic stability in composite wings", *J. Mech. Mater. Struct.* **2**:7 (2007), 1381–1394.

[Maalawi 2002] K. Y. Maalawi, "Buckling optimization of flexible columns", *Int. J. Solids Struct.* **39**:23 (2002), 5865–5876.

[Maalawi and El Chazly 2002] K. Y. Maalawi and N. M. El Chazly, "Global optimization of multi-element beam-type structures", in *The 2nd international conference on advances in structural engineering and mechanics, ASEM02* (Busan, South Korea), August 21–23 2002.

[Rasheed and Yousif 2001] H. A. Rasheed and O. H. Yousif, "Buckling of thin laminated orthotropic composite rings/long cylinders under external pressure", *Int. J. Struct. Stab. Dyn.* **1**:4 (2001), 485–507.

[Rasheed and Yousif 2005] H. A. Rasheed and O. H. Yousif, "Stability of anisotropic laminated rings and long cylinders subjected to external hydrostatic pressure", *J. Aerospace Eng.* **18**:3 (2005), 129–138.

[Reddy 2004] J. N. Reddy, *Mechanics of laminated composite plates and shells: theory and analysis*, 2nd ed., CRC Press, Boca Raton, 2004.

[Simitses 1976] G. J. Simitses, *An introduction to the elastic stability of structures*, Prentice-Hall, Englewood Cliffs, N.J., 1976.

[Simitses 1996] G. J. Simitses, "Buckling of moderately thick laminated cylindrical shells: a review", *Compos. Part B Eng.* **27**:6 (1996), 581–587.

[Soden et al. 1998] P. D. Soden, M. J. Hinton, and A. S. Kaddour, "Lamina properties, lay-up configurations and loading conditions for a range of fibre-reinforced composite laminates", *Compos. Sci. Technol.* **58**:7 (1998), 1011–1022.

[Sridharan and Kasagi 1997] S. Sridharan and A. Kasagi, "On the buckling and collapse of moderately thick composite cylinders under hydrostatic pressure", *Compos. Part B Eng.* **28**:5-6 (1997), 583–596.

[Tanguy et al. 2002] M. Tanguy, P. Mariusz, G. Bernard, and C. Pierre, "Optimal laminations of thin underwater composite cylindrical vessels", *Compos. Struct.* **58**:4 (2002), 529–537.

[Vanderplaats 1994] G. Vanderplaats, *Numerical optimization techniques for engineering design: with applications*, McGraw-Hill, New York, 1994.

[Venkataraman 2002] P. Venkataraman, *Applied optimization with MATLAB programming*, Wiley, New York, 2002.

[Vinson 1992] J. R. Vinson, *The behavior of shells composed of isotropic and composite materials*, Kluwer Academic, Dordrecht, 1992.

[ZitzEvancih 1985] L. D. ZitzEvancih, "Designing graphite cylinders to resist buckling", *AIAA J.* **85** (1985), 1101. Also, *AIAA/SAE/ASME/ASEE* 21st Joint Propulsion Conference, Monterey, CA: July 8–10, 1985.

Received 7 Oct 2007. Revised 21 Jan 2008. Accepted 22 Jan 2008.

KARAM Y. MAALAWI: maalawi@netscape.net
Department of Mechanical Engineering, National Research Center, 12622 Dokki, Cairo, Egypt
www.nrc.sci.eg